Fragment isotope spectra from the ^{36}Ar + Ag reaction at 35 MeV/nucleon

Á. Horváth, F. Deák, and Á. Kiss
Department of Atomic Physics, Eötvös Loránd University, H-1088 Puskin u. 5-7, Budapest, Hungary

Z. Seres
KFKI Research Institute for Particle and Nuclear Physics, H-1525 Budapest 114, Hungary

A. Galonsky, C. K. Gelbke, H. Hama,* L. Heilbronn,† D. Krofcheck‡ W. G. Lynch, D. W. Sackett,§ H. R. Schelin,‖ and M. B. Tsang
National Superconducting Cyclotron Laboratory and Department of Physics and Astronomy, Michigan State University, East Lansing, Michigan 48824

J. Kasagi
Tohoku University, Sendai, Japan

T. Murakami
Kyoto University, Kyoto, Japan
(Received 6 July 1993)

Inclusive fragment isotope spectra were measured at 15°, 30°, 45°, and 60° for the ^{36}Ar + Ag reaction at 35 MeV/nucleon. The energy spectra of many isotopes of elements from Be to Ne were obtained. A two-parameter thermal model fits the angular distributions of the low-energy fragments. One parameter, source kinetic energy/temperature, is proportional to fragment mass number. The other, total fragment production cross section, after adjustment for binding energy, has a decreasing exponential dependence on mass number.

PACS number(s): 25.70.Lm, 25.70.Pq

I. INTRODUCTION

The investigation of fragment production in heavy-ion collisions in the intermediate energy range (30 MeV/$< E/A <$ 500 MeV) has attracted wide interest in recent years [1–7]. Several possible mechanisms for the production of fragments, e.g., evaporation, incomplete fusion, and fragmentation, have been suggested [1–7]. Questions of the interplay between individual nuclear properties of the produced fragments, some combinatorial effects, and the role of multifragmentation are still to be answered.

Double differential cross sections of the isotopes produced from intermediate energy collisions are frequently used sources of information. Experiments investigating fragment spectra from intermediate energy heavy-ion collisions generally show two components—a quasielastic (QE) component whose velocity is centered near the bombarding velocity and a low-energy component whose peak velocity is much lower. These two components belong to different reaction mechanisms which are selected by impact parameter.

Most experimental work in the intermediate energy range gives the dependence of cross section on atomic number. Cross section can also depend on mass number. In order to see this dependence we must measure spectra of individual isotopes. Other fragment parameters that cross section might depend on are Coulomb repulsion energy and fragment binding energy.

This paper presents inclusive double differential cross sections $\partial^2\sigma/[\partial(E/A)\partial\Omega]$ from the ^{36}Ar + Ag reaction at 35 MeV/nucleon for 31 isotopes of Be, B, C, N, O, F, and Ne at 15°, 30°, 45°, and 60° in the energy range 3–40 MeV/nucleon. A parametrization of the low-energy component is presented and discussed.

II. EXPERIMENTAL PROCEDURE

The experiment was performed with the K500 cyclotron of the National Superconducting Cyclotron Laboratory of Michigan State University. The experimental setup is similar to one used earlier [3]. The incident beam was ^{36}Ar at 35 MeV/nucleon with 10^9 ions/s intensity, and a natural silver target of 2.2 mg/cm^2 areal density was used. Silicon detector telescopes were placed in the

*Present address: UVSOR, Institute for Molecular Science, Okazaki, Japan.
†Present address: Lawrence Berkeley Laboratory, Berkeley, CA 94720.
‡Present address: National Lawrence Livermore Laboratory, Livermore, CA 94550.
§Present address: NITON Corporation, 74 Loomis Street, Bedford, MA 01730.
‖Present address: Centro Federal de Educacão Technologica, Av. Sete de Setembro 3165 80230-901, Curitiba, Pr, Brazil.

scattering chamber to detect fragments at 15°, 30°, 45°, and 60°. The telescopes consisted of 2 to 4 elements, the number depending on the angle. The first ΔE detectors were 30 μm in thickness, allowing isotope separation from Z = 4–10 down to E/A = 2–10 MeV, 2 MeV for the lighter fragments and 10 MeV for Z = 10. The second ΔE detectors were 100 μm thick. The E detectors stopped all fragments at least up to 40 MeV/nucleon. The solid angles of the telescopes were about 10 msr. Thin gold foils were placed in front of the telescopes to reduce the number of electrons and x rays from the target. The telescopes were energy calibrated with the aid of a precision pulse generator. Corrections were made for energy loss in the gold foil and half the target event by event. The uncertainty in the fragment kinetic energy measurement was estimated to be typically 2%. We were successful in rejecting the numerous hydrogen and helium nuclei with hardware.

The isotope separation was performed by the ΔE-E standard technique [8]. In all cases elements were easily separated. For each element a two-dimensional energy-particle identification spectrum was constructed. These spectra were sliced into channels 0.5 MeV/nucleon wide. The resulting one-dimensional particle identification spectra were then fitted with Gaussians of a single width for each isotope having significant intensity; linear background was included.

III. EXPERIMENTAL RESULTS

We identified 31 isotopes of Be, B, C, N, O, F, and Ne. We saw a small amount of sodium and magnesium isotopes as well, but only at 15°.

Double differential cross sections were determined. In Fig. 1 we present typical spectra at 15°, 30°, 45° and 60°. In the spectra at 15° there are two main components. A bump not far below the projectile velocity comes from QE reactions, and the lower energy part from a strongly damped reaction. The QE bump is asymmetric with a low energy tail, corresponding to significant damping. It shows features discussed in [2,3]. In those papers it was suggested that the QE bump resulted from a fragmentationlike process followed by interaction with hot nuclear matter.

At 15° and 30° the spectra were decomposed into the two components according to a slight variation of the method of [3]. In Fig. 1 in the top two rows, the dashed and the dot-dashed lines show the QE and low-energy components separately, and the solid line shows the sum of the two. At 30° the contribution of the QE component to the spectra is less than ten percent. At larger angles (Fig. 1, lower two rows) the spectra are fitted with only one component, and that component shows an almost exponential decrease with energy. There is an unseen contribution below the detection thresold in every spectrum. Our estimates of the average amount of this contribution are 1%, 2%, 4%, and 10% at 15°, 30°, 45°, and 60°, respectively.

For the low-energy component, we integrated the spectra to produce values of $d\sigma/d\Omega$ at each of the four angles. The errors of these energy-integrated cross sections are determined by the errors of the double differential cross section data, by the uncertainities of the separation into

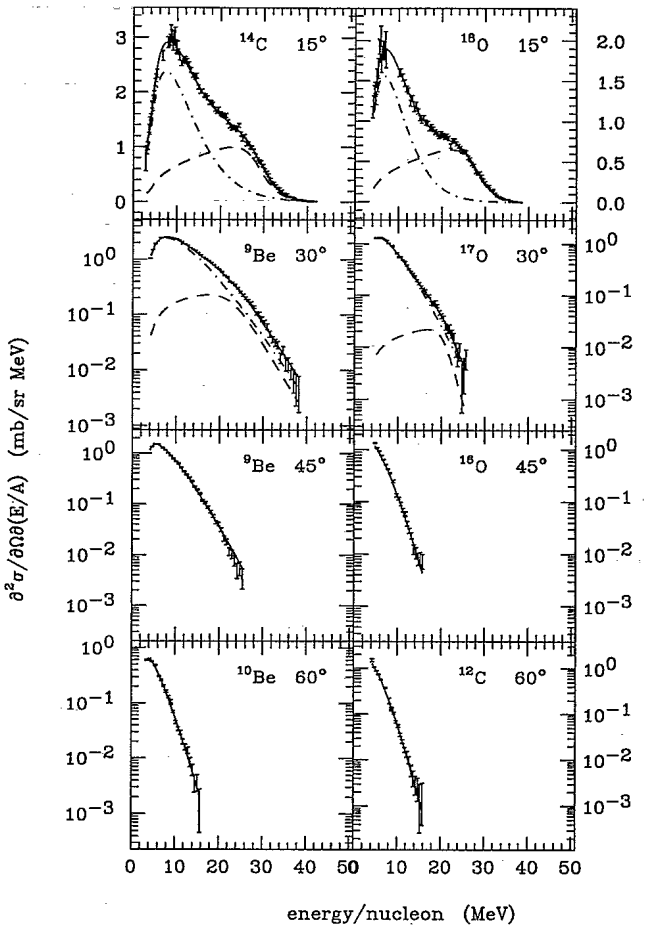

FIG. 1. Fragment energy spectra for several isotopes at the indicated angles. The dashed curves show the contribution of the QE component, and the dot-dashed curves show the contribution of the low-energy component.

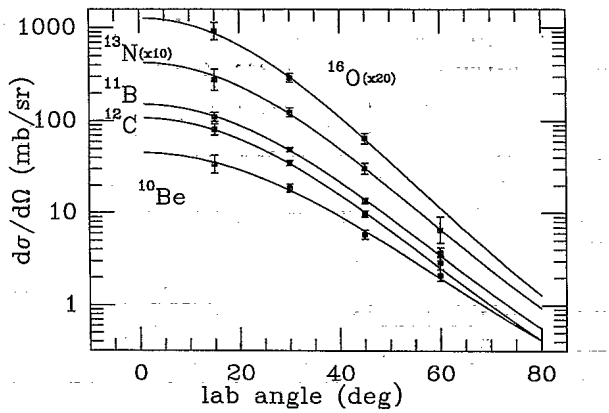

FIG. 2. The angular distribution of the energy-integrated cross section for the low-energy component for several representative isotopes. The solid curves show the fits to the data of a thermal equilibrium model.

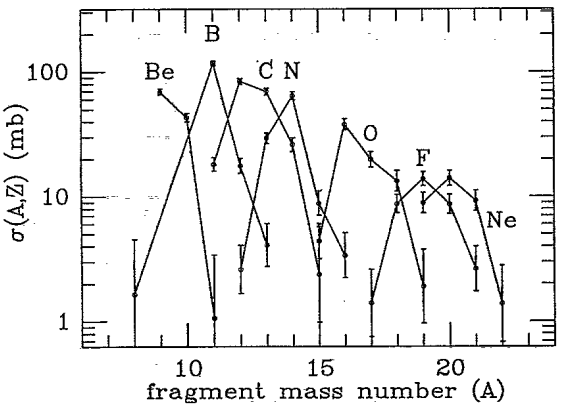

FIG. 3. The dependence on the fragment mass number of the amplitude parameter of a thermal model. These amplitude values are the total cross sections for production of the indicated fragments. The values which correspond to isotopes of the same element are connected by solid lines.

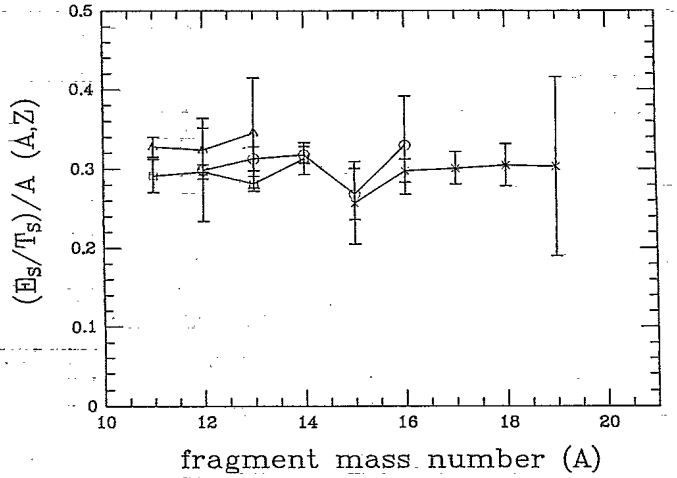

FIG. 4. The dependence on fragment mass number of the E_S/T_S (shape) parameter divided by A of a thermal model. This combination appears to be the same for all fragment species. The values which correspond to isotopes of the same element are connected by solid lines.

two components at 15° and 30°, and by the contributions below threshold. For each isotope the angular distribution data show a smooth falloff with angle. Figure 2 shows a sampling of these angular distributions along with fitted curves discussed next.

To determine the total cross sections $\sigma(Z,A)$ of the low-energy component, we fitted the angular distribution data using the shape function of the moving source model:

$$\frac{d\sigma(Z,A)}{d\Omega}(\vartheta) = \sigma(Z,A)\int_0^\infty \frac{1}{2\pi^{\frac{3}{2}}T_S^{\frac{3}{2}}}\sqrt{E}\exp\left(-\frac{E+E_S-2\sqrt{EE_S}\cos\vartheta}{T_S}\right)dE. \tag{3.1}$$

Here E is the laboratory kinetic energy of the fragment; the parameter corresponding to the velocity of the source $E_S = \frac{1}{2}Am_0v_S^2$, where m_0 is the nuclear mass unit and v_s is the source velocity; T_S is the temperature parameter; and $\sigma(Z,A)$ is the total cross section for production of the (Z,A) isotope. The integral uses the error function with argument $\cos\vartheta$. (We note that after integration, E_S and T_S appear only as the quotient E_S/T_S.) The curves in Fig. 2 show the fits to the data for several isotopes. The fitting parameters were E_S/T_S and $\sigma(Z,A)$.

Figure 3 shows the values of total cross section obtained in this way for all 31 isotopes. The points for isotopes of the same element are connected by straight lines.

IV. DISCUSSION OF RESULTS

We found that the values of each of the fit parameters, E_S/T_S and $\sigma(Z,A)$, for the various fragments of the low-energy component obey a regularity as a function of A. E_S/T_S is approximately proportional to A. This can be seen in Fig. 4 where $(E_S/T_S)/A \simeq 0.303 \pm 0.015$. This result can be interpreted as support for an evaporation model in which the value of the temperature parameter is nearly constant for the different isotopes. To estimate that value, we assume central collisions for the reaction mechanism producing the low-energy fragments. Then the source velocity is the same for all fragments, viz., $v_S(A,Z) \simeq v_{\text{c.m.}}$. Therefore, $E_S \simeq \frac{1}{2}Am_0v_{\text{c.m.}}^2 = A$ (2.19 MeV), and the value of E_S/A is also the same for all fragments. From the constancy of $(E_S/A)/T_S$ we can conclude that the temperature parameter T_S is also constant, and it has the value 7.2 ± 0.7 MeV. A constant

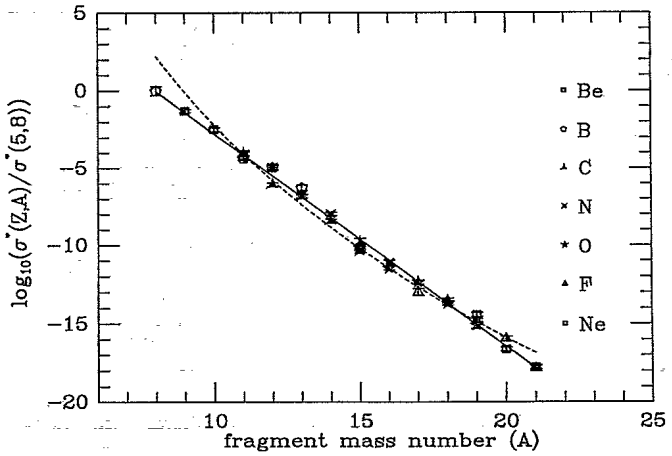

FIG. 5. The dependence of the reduced (for binding energy) cross section for fragment production σ^* relative to σ^* for ^{8}B. The solid line represents the best exponential fit to the corrected cross sections, and the dashed curve is the best power law fit to the same data.

temperature is consistent with the thermal behavior of the fragment angular distributions.

The regularity of $\sigma(Z,A)$ is not as apparent. The fragment cross sections in Fig. 3 show maxima for the isotopes with the greatest binding energy per nucleon. Hirsch *et al.* [1], and others, have shown how fragment production cross sections depend on binding energy. Therefore, we created values of $\sigma^*(Z,A) = \sigma(Z,A)/\exp(E_{\text{binding}}/T_S)$ using the known values of the binding energies [10] and 7.2 MeV for T_S. In Fig. 5 we see the regularity—the dependence of $\sigma^*(Z,A)$ on A is almost exponential.

The data in Fig. 5 show that when corrected for binding energy the large dependence of $\sigma(Z,A)$ on Z in Fig. 3 almost disappears. The important parameter for the probability of producing a fragment with a given mass number is the binding energy, not another parameter such as the Coulomb energy. The exponential dependence on A is what is expected if evaporation is the dominant fragment production mechanism [9]. Multifragmentation leads to a power-law rule $\sigma^*(Z,A) \sim A^{-\kappa}$ as studied and suggested in [1,9]. We fitted the data in Fig. 5 with both forms and found that the χ^2 per degree of freedom was 7 for the exponential (solid line) and 21 for the power law (dashed curve), a result that favors evaporation over multifragmentation.

ACKNOWLEDGMENTS

The authors wish to thank the cyclotron crew at the NSCL for providing good beam. This work was supported in part by NSF Grants PHY92-14992 and INT91-13997, by the Hungarian Academy of Science, and by the CNPq-Brazil.

[1] A.S. Hirsch, A. Bujak, J.E. Finn, L.J. Gutay, R.W. Minich, N.T. Porile, R.P. Scharenberg, and B.C. Stringfellow, Phys. Rev. C **29**, 508 (1984).

[2] Z. Seres, F. Deák, Á. Kiss, A. Galonsky, and L. Heilbronn, Nucl. Phys. **A492**, 315 (1989).

[3] Á. Kiss, F. Deák, Z. Seres, G. Caskey, A. Galonsky, B. Remington, and L. Heilbronn, Nucl. Phys. **A499**, 131 (1989).

[4] M.C. Etchegoyen, A. Etchegoyen, A.O. Macchiavelli, G. Crawley, C. Djalali, M. Renteria, A. Szanto de Toledo, and G. Westfall, Nucl. Phys. **A518**, 572 (1990).

[5] B. Borderie, M. Montoya, M.F. Rivet, D. Jouan, C. Cabot, H. Fuchs D. Gardes, H. Gauvin, D. Jacquet, and F. Monnet, Phys. Lett. B **205**, 26 (1988).

[6] B.V. Jacak, G.D. Westfall, G.M. Crawley, D. Fox, C.K. Gelbke, L.H. Harwood, B.E. Hasselquist, W.G. Lynch, D.K. Scott, H. Stöcker, M.B. Tsang, and G. Buchwald, Phys. Rev. C **35**, 1751 (1987).

[7] F. Rami, J.P. Coffin, G. Guillaume, B. Heusch, P. Wagner, A. Fahli, and P. Fintz, Nucl. Phys. **A444**, 325 (1985).

[8] T. Shimoda, M. Ishihara, and K. Nagatani, Nucl. Instrum. Methods **165**, 261 (1979).

[9] W. Bauer, Phys. Rev. C **38**, 1297 (1988).

[10] Handbook of Chemistry and Physics 72nd edition (CRC, Boca Raton, FL, 1991, 1992).